$$f_1(\bar{x},\bar{y}) = A_{00} + A_{20}\bar{x}^2 + A_{02}\bar{y}^2 + A_{40}\bar{x}^4 + A_{22}\bar{x}^2\bar{y}^2 + A_{04}\bar{y}^2 + A_{42}\bar{x}^4\bar{y}^2 + A_{24}\bar{x}^2\bar{y}^4 + A_{44}\bar{x}^4\bar{y}^4 \quad (11)$$

2) for modes antisymmetric about the x axis and symmetric about the y axis:

$$f_3(\bar{x},\bar{y}) = A_{10}\bar{x} + A_{30}\bar{x}^3 + A_{12}\bar{x}\bar{y}^2 + A_{50}\bar{x}^5\bar{y} + A_{32}\bar{x}^3\bar{y}^2 + A_{14}\bar{x}\bar{y}^4 + A_{52}\bar{x}^5\bar{y}^2 + A_{34}\bar{x}^3\bar{y}^4 + A_{54}\bar{x}^5\bar{y}^4 \quad (12)$$

The actual solution to the buckling problem is the one of these two expressions which yields lower values for $N\bar{x}$ and $N\bar{y}$. Since only the lowest eigenvalue of Eq. (9) that corresponds to the critical load is of interest, the iterative collocation least-square scheme is the most appropriate. The iteration process begins with $N = N\bar{x} = rN\bar{y} = 0$, where r is the ratio $N\bar{x}/N\bar{y}$ and the iteration ceases when

$$|N_n - N_{n-1}| / |N_n| = 10^{-5} \quad (13)$$

where N_n is the eigenvalue after n cycles of iteration. In all cases, this accuracy is reached within five iterations.

Results and Conclusions

Results for the buckling of clamped rectangular plates using this analysis are tabulated in Table 1. Comparisons of results are made with values obtained by Timoshenko and Gere[8] for the case of biaxial compression and by Levy[9] and Maulbetsch[10] for the case of uniaxial compression. As can be seen in Table 1, the present results are in excellent agreement with the accurate Fourier series solution reported by Levy.[9] The Ritz solutions reported by Maulbetsch[10] and Timoshenko and Gere[8] appear to be the upper bound of the maximum percentage difference between these values and the present result is less than 2.5%. Figure 2 shows plots of simultaneous critical buckling loads $N\bar{x}$ and $N\bar{y}$ for aspect ratios $R = a/b$ ranging rom 1 to 2. These curves are called interaction curves. It can be seen from the figure that the point of intersection of an interaction curve with the x axis gives the critical value of Nx for the case where $Ny = 0$. The intersection of the same curve with the y axis gives the critical value of Ny when $Nx = 0$. For the case $Nx = Ny = N_0$, the critical buckling load N_0 is determined by the intersection of these curves with the line which goes through the origin 0 of the coordinate system and makes an angle of 45 deg with the horizontal axis.

The buckled shape of the plate under a given combination of Nx and Ny for a particular value of a/b is also indicated in Fig. 2 where m is the number of half-waves in the x direction and n is the number of half-waves in the y direction.

From the results presented herein, it can be concluded that the distinct advantage of the least-square augmented collocation method lies in the fact that it completely eliminates the need for the tedious process of integration generally associated with the Galerkin or Ritz type of solution. Furthermore, in addition to its simplicity in mathematical formulation, the collocation least-square method has been demonstrated to yield accurate results that converge rapidly and such results are independent of the location and distribution of collocation points.

Acknowledgment

This work was sponsored by the National Research Council of Canada under Grant A-4357.

References

[1] Gerard, G. and Becker, H., "Handbook of Structural Stability, Pt. I: Buckling of Flat Plates," NACA TN 3781, 1957.

[2] Flugge, W., *Handbook of Engineering Mechanics*, McGraw-Hill Book Co., N.Y., 1962.

[3] Ng, S. F., "A Collocation Least Square Solution of Boundary Value Problems in Applied Mechanics," *Proceedings of the Symposium on Computer Aided Engineering*, University of Waterloo, Canada, May 1971, pp. 395-402.

[4] Ng, S. F. and Chan, M.Y.T., "Solution of Some Boundary Value Problems in Applied Mechanics by the Collocation Least Square Method," *Journal of Computer Methods in Applied Mechanics and Engineering*, Vol. 11, No. 2, May 1977, pp. 137-150.

[5] Frazer, R. A., Jones, W. P., and Skan, S. W., "Approximation of Function and to the Solution of Differential Equations," Aerodynamics Dept. N.P.L., R&M 1799, March 1937.

[6] Collatz, L., *The Numerical Treatment of Differential Equations*, Springer, Berlin, 1960, pp. 409-413.

[7] Timoshenko, S. and Woinowsky-Krieger, S., *Theory of Plates and Shells*, McGraw-Hill Book Co., N.Y., 1959.

[8] Timoshenko, S. and Gere, J., *Theory of Elastic Stability*, 2nd ed., McGraw-Hill Book Co., N.Y., 1961.

[9] Levy, S., "Buckling of Rectangular Plates with Built-In Edges," *Journal of Applied Mechanics*, Vol. 9, Dec. 1942, pp. 171-174.

[10] Maulbetsch, J. L., "Buckling of Compressed Rectangular Plates with Built-In Edges," *Journal of Applied Mechanics*, Vol. 59, 1937, p. 59.

Influence of Suction on the Developing Wall Flow of an Impinging Jet

N. T. Obot,* W.J.M. Douglas,† and A. S. Mujumdar‡
McGill University, Montreal, Canada
and
Pulp and Paper Research Institute of Canada, Pointe Claire, Quebec, Canada

Introduction

ALTHOUGH impinging jet flows have been studied extensively, little information exists on the effects of applying moderate suction along the surface of the developing flows.[1,2] The imposition of suction along the impingement surface is an inherent feature of any drying installation utilizing a combination of impingement and through flow—a process whereby an impinging hot gas is drawn through the moist permeable web by means of suction. This work stems from the need to obtain experimental information on the flowfield that would be helpful in interpretation of the role of suction on impingement heat transfer.[3]

Experimental Facility and Procedures

The room temperature uniform jet issuing from a 20 mm diam (d_n) contoured inlet nozzle impinged concentrically on a 0.97 m diam plate of which the flush-mounted central section, 348 mm diam and 9.5 mm thick, was of porous Tegraglas. The nozzle, machined according to ASME standards, had elliptical inlet and square-edged exit sections. Tegraglas porous (product of 3M Company) plate was chosen because of its excellent surface smoothness and uniform permeability. The outer ring of plexiglass served as an extended surface for jet flow away from the test section. The permeable test plate was mounted in a suction box with its top surface flush with the edges of the suction box. The small clearance between the walls of the suction box and the end of the test plate was filled

Received March 15, 1982; revision received Oct. 4, 1982.

*Research Assistant; presently, Assistant Professor, Department of Chemical Engineering, Clarkson College of Technology, Potsdam, N.Y.

†Professor and Head, Department of Chemical Engineering.

‡Associate Professor, Department of Chemical Engineering.

with plasticine. A 19 mm wide strip of transparent Scotch tape, placed over the plasticine and in contact with both the edges of the test plate and of the suction box, prevented flow through this area when suction was applied. Forty-one miniature flush-mounted pressure taps, 33 of which were located along the main traverse diameter (x axis) and the remaining along the y axis, facilitated establishment of flow symmetry along the test plate. Suction under the test plate was provided by a centrifugal blower. The flow rate of the air withdrawn through the test plate was measured with a calibrated orifice installed in the suction line.

Measurements of mean velocity were made using a DISA constant-temperature anemometer (55M01), the output of which was linearized by means of an electronic linearizer (DISA 55D10). Boundary-layer gold-plated probes (type 55P05) were used. Distances within the inner region adjacent to the surface were measured in increments of 0.5 mm, but in coarser intervals in the outer region. The worst possible error associated with measurement of the distances is no more than 8%. The jet Reynolds number was fixed at 80,000, i.e., corresponding to nozzle exit average velocity of 60 m/s. Additional information on the experimental program is available in Ref. 1.

Results and Discussion

A brief comment prior to discussion of the figures concerns variations in the suction velocity V_w along the test plate. Since through flow is achieved by maintaining a uniform reduced pressure on the suction side of the test plate, it is unavoidable that, because the impingement surface pressure decreases radially from its maximum at the stagnation point, local through flow must also vary in a similar manner. It is known that small surface pressure variations can produce local inflows and outflows.[4] Preliminary tests[1] revealed no inflows, probably because of the low permeability and the large thickness of the test plate.

Figure 1 shows plots of the velocity distribution obtained at two radial locations, $r=80$ and 120 mm, measured from the stagnation point for $Z_n/d_n=12$. Of the several trends that may be noted on this figure, one that is readily predictable intuitively is that suction reduces the boundary-layer thickness [i.e., distance from plate ($y=0$) to the location of U_m] and correspondingly increases the velocity gradient near the wall. The trend that is not so directly predictable is that U_m is increased in every case. Both of these effects combine to increase the wall shear stress. Another feature is that the velocity profiles with suction cross those without. This consequence of continuity is not altogether surprising for it can be argued that, even if the total radial volumetric flow rate were unchanged, any modification causing the velocity to be increased near the wall must be compensated by a reduction far from the wall. All of the characteristics noted above were in clear evidence at all spacings and radial locations studied.

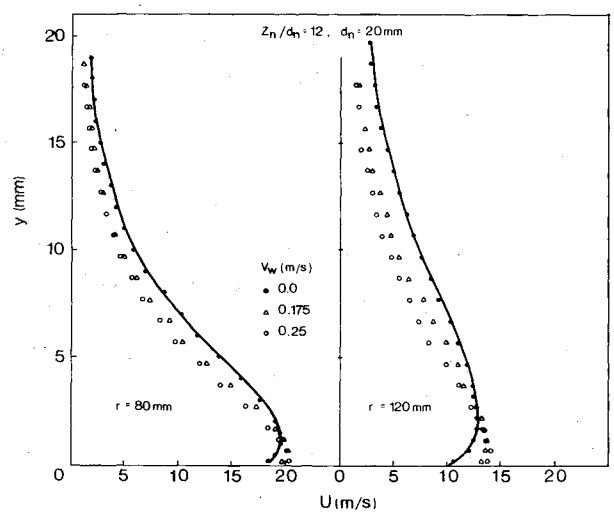

Fig. 1 Effect of suction on radial mean velocity distribution at $Z_n/d_n=12$.

Figures 2 and 3 are dimensionless plots of velocities obtained at two radial locations for $H=3$ and 8, respectively. The abscissa on each plot represents the height y above the impingement surface measured in terms of $\delta_{1/2}$, where $U(\delta_{1/2})=\frac{1}{2}U_m$ and U_m is the maximum velocity. The theoretical curve of Glauert[5] (for $\alpha=1.3$) is shown on each plot, while the experimental profiles at the 4 d_n distance from the stagnation point (Fig. 3a) are compared with the $r/Z_n=0.18$ results of Bradshaw and Love.[6] It is useful to note that the $r=80$ and 120 mm locations may be stated, respectively, as $r/Z_n=1.33$ and 2 for $Z_n/d_n=3$ (Fig. 2), and as $r/Z_n=0.5$ and 0.75 for $Z_n/d_n=8$ (Fig. 3).

Figure 2 establishes that, except very close to the impingement surface, the no-suction results are adequately represented by Glauert's profile for $y/\delta_{1/2}<1.2$, in line with the results of Poreh et al.,[7] which showed that for $r/Z_n>0.75$ profiles obtained at all radial locations collapsed into a single curve. The present $V_w=0$ results together with those of Ref. 6 provide justification for the conclusion that, for $0<y/\delta_{1/2}<1$, the lower the r/Z_n value, the larger the deviation of the experimental profile from Glauert's theoretical curve. The consequence of applying moderate suction is clearly evident and, in fact, the results follow two distinct trends, one for $r/Z_n\geq 1.33$ (Fig. 2) and the other for $r/Z_n\leq 0.75$ (Fig. 3). For $r/Z_n\geq 1.33$ the dimensionless profiles are not only independent of both the suction velocity and radial location, but also exhibit little departure from Glauert's theoretical curve for $0<y/\delta_{1/2}<1$. In the latter case, since the $V_w=0$ profiles for $r/Z_n\leq 0.75$ vary with radial location, it is not surprising that the profiles show mild dependence on location and suction velocity. Further, the profiles with suction deviate from those without suction.

Figure 4 provides additional information on the effects of varying V_w on U_m (in m/s) and $\delta_{1/2}$ (in mm). The horizontal

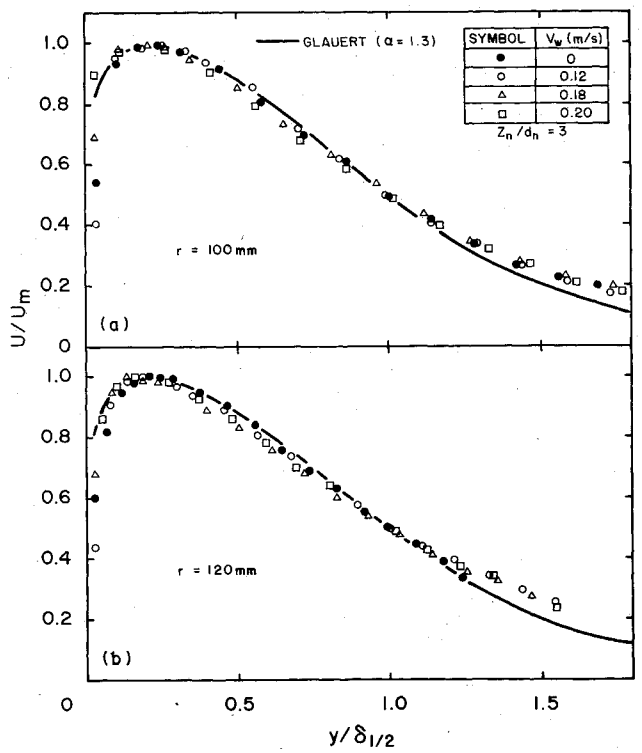

Fig. 2 Effect of suction on dimensionless velocity profiles at $Z_n/d_n=3$.

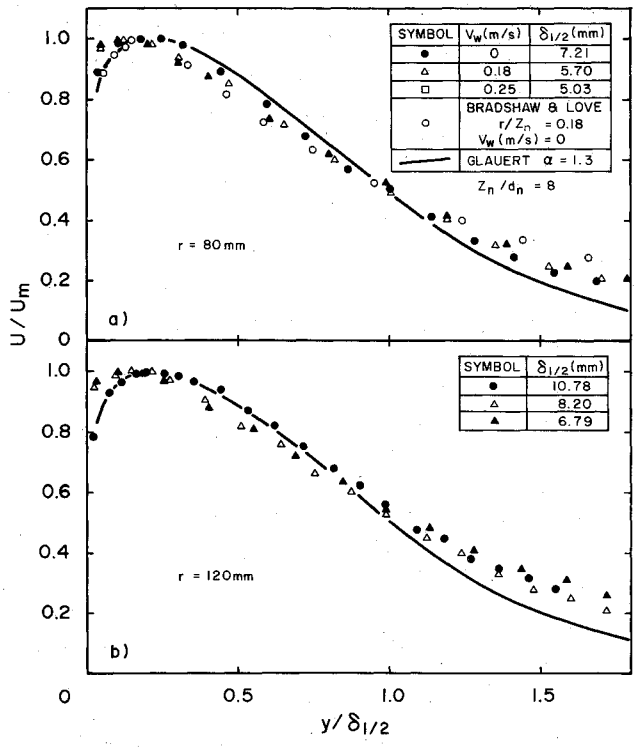

Fig. 3 Effect of suction on dimensionless velocity profiles at $Z_n/d_n=8$.

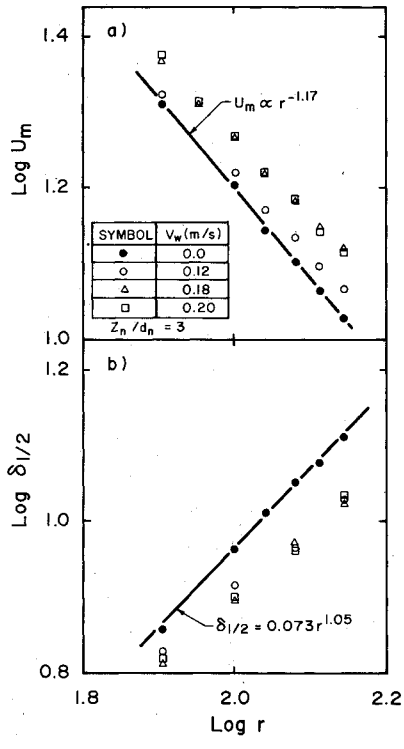

Fig. 4 Effect of suction on maximum velocity and wall jet half-width at $Z_n/d_n=3$.

axis r is in millimeters. The numercial values of the exponent quoted on these plots correspond to the least square estimated inclination of a straight line through the points for $V_w=0$.

Figure 4a shows that the absolute increase in U_m does not vary greatly with r. It is of some interest to note that, for impingement on an impermeable surface, Glauert's theoretical prediction gave $U_m \propto r^{-1.14}$, while the experimental studies of Refs. 8 and 9 resulted in exponents on r of -1.12 and -1.122, respectively, all of which are close to the present value of -1.17.

From Fig. 4b it may be noted that the suction reduces $\delta_{1/2}$ by roughly a constant amount, in sharp contrast with the trend tabulated on Fig. 3 for $Z_n/d_n=8$. In general, for a given radial location and suction velocity, the magnitude of the reduction in $\delta_{1/2}$ was found to increase with increasing spacing, indicating a more intense effect of suction at large spacings. This trend was also reflected in heat transfer results reported in Ref. 3. For $V_w=0$, $\delta_{1/2}$ was found to be essentially independent of Z_n/d_n over the range of radial locations ($4 \le r/d_n \le 7.5$) studied. For instance, at $r/d_n=6$ and for $Z_n/d_n=3$, 8, and 12, $\delta_{1/2}$ values are (in the same order) 11.28, 10.78, and 11.25 mm. It is also of some interest to note that, for $V_w=0$, $\delta_{1/2} \propto r^n$ (where $n=1.05$), which is close to Glauert's value of 1.02 for $\alpha=1.3$.

Baines and Keffer[2] investigated the effect of suction on the boundary-layer characteristics due to normal impingement of a slot jet on a stationary surface. Their results do not modify the conclusions of the present study. Specifically, application of suction equivalent to 0.29% of the nozzle exit average velocity displaced the boundary layer closer to the impingement surface and caused about a 4% increase in U_m at about 15 slot widths downstream from the stagnation point.

Conclusion

Suction creates a larger volume of flow toward the impingement surface, reduces the momentum boundary-layer thickness and the wall jet half-width, and increases velocity gradient near the surface and hence the wall shear stress. For $r/Z_n \ge 1.33$, the dimensionless velocity profiles are independent of both suction velocity and radial location.

References

[1]Obot, N. T., "Flow and Heat Transfer for Impinging Round Turbulent Jets," Ph.D. Thesis, McGill University, Montreal, Canada, 1980.

[2]Baines, W. D. and Keffer, J. F., "Shear Stress Measurements for an Impinging Jet—Effects of Surface Motion and Suction," Pulp and Paper Research Institute of Canada, Tech. Rept. PPR/186, 1977.

[3]Obot, N. T., "Effect of Suction on Impingement Heat Transfer," *Proceedings of the 7th International Heat Transfer Conference*, Vol. 3, 1982, pp. 389-394.

[4]Squire, L. C., "Comment on 'Turbulent Bounary Layer with Injection and Surface Roughness'," *AIAA Journal*, Vol. 16, June 1978, pp. 639-640.

[5]Glauert, M. B., "The Wall Jet," *Journal of Fluid Mechanics*, Vol. 1, Pt. 6, Dec. 1956, p. 625-643.

[6]Bradshaw, P. and Love, E. M., "The Normal Impingement of a Circular Jet on a Flat Plane," Great Britain Aeronautical Research Council, R&M 3205, Sept. 1959.

[7]Poreh, M., Tsuei, Y. G., and Cermak, J. E., "Investigation of a Turbulent Radial Wall Jet," *Journal of Applied Mechanics*, Vol. 89, June 1967, pp. 457-463.

[8]Bakke, P., "An Experimental Investigation of a Wall Jet," *Journal of Fluid Mechanics*, Vol. 2, Pt. 5, July 1957, pp. 467-472.

[9]Govindan, A. P. and Subba Raju, K., "Hydrodynamics of a Radial Wall Jet," *Journal of Applied Mechanics*, Vol. 41, No. 2, June 1974, pp. 518-519.